33ND INTERNATIONAL COSMIC RAY CONFERENCE, RIO DE JANEIRO 2013
THE ASTROPARTICLE PHYSICS CONFERENCE

ICRC 2013

The impact of cosmic ray transport scenarios on the local positron fraction

IRIS GEBAUER[1], SIMON KUNZ[1], MATTHIAS WEINREUTER[1].

[1] *Karlsruhe Institute of Technology, D-76131 Karlsruhe, Germany*

gebauer@kit.edu

Abstract: The rising positron fraction, as measured by PAMELA, Fermi and most recently AMS-02, requires an energetic positron population in addition to the secondary positrons produced in cosmic ray interactions in the interstellar medium. Possible explanations are local astrophysical sources such as pulsars, supernova remnants or more exotic sources such as dark matter. In all cases the additional positron contribution crucially depends on the galactic background model, which determines the relative contribution of secondary positrons from cosmic ray interactions and on the specific transport parameters in the solar neighborhood. The latter is of particular importance for high energy positrons due to their large energy losses and therefore short propagation lengths. Based on a full numerical solution to the transport equation we estimate the uncertainties of the background model due to variations in the transport parameters. The model incorporates a realistic treatment of the local environment of our Sun, as well as the galactic spiral arms and allows for radially varying galactic wind strengths as expected from the ROSAT observations. The global transport parameters have been fixed by a set of independent observables (protons, antiprotons, ratios of secondary to primary isotopes and ratios of radioactive isotopes). We show the resulting uncertainties in the local cosmic ray spectra, positron fraction and comment on the implications for diffuse γ-rays.

Keywords: galactic cosmic rays, local bubble, spiral arms, DRAGON, pulsars, positron fraction, AMS-02

1 Introduction

Galactic cosmic rays (CR) are believed to be produced in supernova remnants (SNRs) throughout the Milky Way. Upon injection into the interstellar medium (ISM) they scatter on magnetic turbulences, leading to a random walk which can be modelled by diffusion. In addition to diffusion, other transport processes, such as diffusive reacceleration, convection due to the common movement of the scattering centers out of the galactic plane, energy losses, fragmentation and particle losses via escape from the galaxy, modify the inital CR spectra on their way to Earth. This process can be described by a diffusion-convection equation, as implemented in the publicly available GALPROP [1] or DRAGON [2] codes. Both programs solve the diffusion-convection equation in steady-state, using a realistic treatment of the galactic gas distribution and the magnetic and interstellar radiation field. The obtained models successfully describe most locally measured CR spectra, however, they fail to interlink the locally observed proton spectra with the galactic averaged proton spectra as observed via the diffuse γ-rays. For instance, the spectrum of diffuse γ-rays tends to prefer a proton spectrum, slightly harder than the one locally measured. Similarly the radial gradient of diffuse γ radiation seems to be incompatible with standard diffusion models, since it requires either an artificially flattened source distribution or non-standard transport setups [3, 4]. The question of the connection between local and global transport phenomena is intimately related to the explanation of the rising positron fraction as observed by PAMELA [5] and most recently by AMS-02 [6]. This excess clearly requires an additional hard positron population, which has been proposed to be produced in pulsars, SNRs or via the decay or annihilation of dark matter particles. Such high energy positrons suffer large synchrotron and inverse Compton losses, which limit their propagation length to the sub-kpc range and consequently make them sensitive to only the local transport modes. Usually transport models try to explain all observables at once by means of averaged transport parameters. This, however, comes at the cost of accuracy and limits the predictive power of such models. Here we pursue a different approach. We use the locally measured proton spectrum, the $\bar{p}/p$, B/C and $^{10}Be/^{9}Be$ ratio to constrain the *global galactic* transport parameters. Protons suffer energy losses predominantly via ionization and Coulomb losses leading to large energy loss times and above-kpc transport lengths. The B/C ratio in combination with the $^{10}Be/^{9}Be$ ratio is a measure for the CR interaction rate and the CR escape time. The $\bar{p}/p$ ratio is an independent measure of the CR interaction rate at higher energies. We employ Markov chain monte carlo (MCMC) to determine the optimal set of transport parameters for these observables. This is descibed in section 2. The so obtained transport parameters fix the globally averaged proton spectrum leading to the known mismatch in diffuse γ-rays. Here we assume that this discrepancy can be attributed to two structures, which are not accounted for by the standard models for galactic CR transport: the local bubble, an underdense region surrounding the Sun and the spiral arm structure of the Milky Way. In sections 2.1 and 2.2 we give a first estimate of the impact of these structures under simple assumptions. In section 3, we compare our best fit model to the AMS-02 data on the positron fraction and comment on the uncertainties in the local pulsar contribution. The results are summarized in section 4 and an outlook is given.

2 Background model and uncertainties

We employ a model with a constant and isotropic diffusion coefficient and a radial dependence of convection velocity proportional to the source strength of CRs. The latter is expected from the ROSAT observations of hot gas at high galactic latitude [7, 8]. The model depends on 16 free parameters describing diffusion, convection, diffusive reacceleration, the halo height, beyond which free escape of particles is assumed, and the proton injection spectrum. In order to examine the full potential of these kind of models and their limitations, a MCMC method was used, to explore the 16 dimensional parameter space of transport parameters. MCMC sampling of the transport parameter space has been performed in the past [9, 10] in simpler models. Here we follow a similar recipe as [9], however, we incorporate the more efficient Multiple-Try-Metropolis algorithm [11]. This algorithm accounts for the dimensionality of the problem by evaluating several models in parallel. In total 10.72 million models have been evaluated. For each of these models the full transport equation as given in, e.g. [12], including energy losses and diffusive reacceleration, was solved numerically using the DRAGON code. Two different sets of Markov chains were run: a first set using constraints from the local proton spectrum, $\bar{p}/p$ and B/C measurements ($6 \cdot 10^6$ evaluated models) and a second set using additional constraints from the $^{10}Be/^{9}Be$ ratio ($4 \cdot 10^6$ evaluated models). Here we report on the results of the second set of chains, which includes the constraints on the CR escape time. Details on the method and the results derived from the full statistics will be presented elsewhere [13].

The best fit to the proton spectrum and the $\bar{p}/p$, B/C and $^{10}Be/^{9}Be$ ratio is shown in figs. 1 and 2 as the black line. Also shown as the blue band is the envelope derived from the top 100 models. A full statistical analysis will be presented elsewhere[13]. A compilation of the most important transport parameters can be found in table 1. The so obtained model reproduces the known discrepancy between the locally observed proton spectral index and diffuse γ-rays: while the best fit model has a proton spectral index of 2.74 for energies above 40 GeV, compatible with the PAMELA data, the Fermi diffuse γ-ray data prefer a proton spectral index of 3.14 between 20 and 200 GeV.

In addition to the uncertainties of the *global galactic* transport model, the Milky Way comprises several short-scale structures which are not implemented in the standard transport models, but are expected to have a significant impact on the transport of galactic CRs and consequently the production of diffuse γ-rays. Two of these structures, the Milky Way's spiral arms and the local bubble, will be discussed in the following subsections.

2.1 Uncertainties from spiral arms

We included a simple spiral arm model into the DRAGON code. The source and gas distributions are taken to directly follow the spiral arm structure as given in [21], while keeping the total gas mass constant and the relative contributions of the different gas components as a function of galactocentric radius unchanged. The impact on proton spectrum, $\bar{p}/p$, B/C and $^{10}Be/^{9}Be$ ratio is summarized in figs. 1 and 2. If the gas distribution follows the spiral arms we see a strong decrease in the secondary production rate. The local secondary flux as given by $\bar{p}$, B and e^+ decreases by a factor 10 at energies below 10 GeV, the isotopic beryllium ratio is reduced by a factor 2 for energies below 100 GeV, indicating a much older CR population compared to the standard gas distributions. This is understandable from

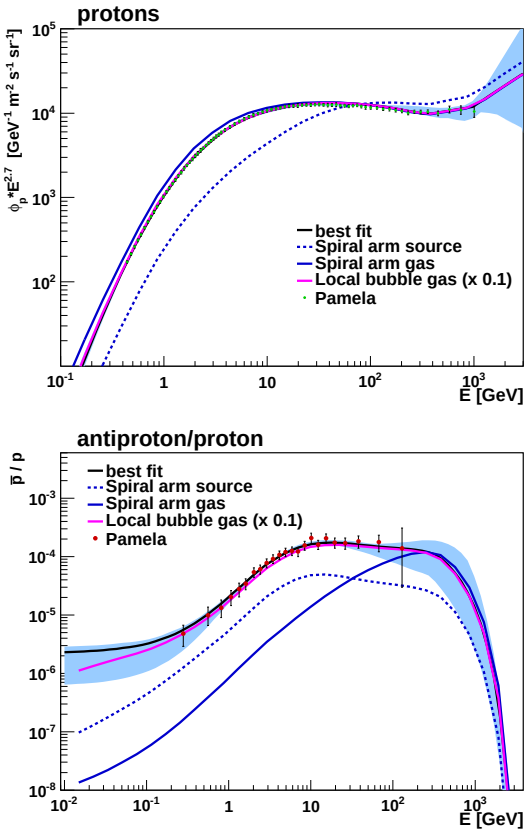

Figure 1: The proton flux (*top*) and antiproton/proton ratio (*bottom*) for the best fit model (*full black line*). The *blue* band refers to the uncertainty from the *global galactic* transport model as described in section 2. It is given by the top 0.001 % of the models (i.e. 100 runs). The *full blue* line shows the best fit model with the interstellar gas distributed along the spiral arms, the *dashed blue* line shows the best fit model for CR sources distributed along the spiral arms (for details see section 2.1). The *full magenta* line shows the best fit model with the gas density inside the local bubble reduced by a factor of 0.1 (see section 2.2 for details). Data from PAMELA [14] (protons) and [15] (antiprotons/protons).

Parameter	best fit	lower limit	upper limit
D_0 $[\frac{cm^2}{s}]$	$1.35 \cdot 10^{28}$	$4.0 \cdot 10^{27}$	$7.0 \cdot 10^{28}$
$\delta_{low}/\delta_{high}$	0.84/0.13	0.47/0.005	1.2/1.2
ρ_0 $[GV]$	972.4	106.5	3488
L $[kpc]$	6.59	1.70	30.0
v_α $[\frac{km}{s}]$	16.57	0.61	40.28
V_0 $[\frac{km}{s}]$	0.17	0.005	29.39
dV/dz $[\frac{km}{s\,kpc}]$	22.7	1.93	50.04
α_r	1.0	0.0012	1.0

Table 1: The best fit values of the most important transport parameters and the limits given by the minimum and maximum value of the respective transport parameters from the top 100 models. D_0: strength of diffusion coefficient at a reference rigidity of ρ_0, $\delta_{high/low}$: rigidity dependence of the diffusion coefficient above/below ρ_0, L halo height, v_α Alfven velocity, V_0 strength of the galactic wind in the plane, dV/dz vertical increase of wind velocity, α_r coupling strength between wind velocity and radial dependence of the source distribution $Q(R)$: $V(R) \propto Q(R)^{\alpha_r}$.

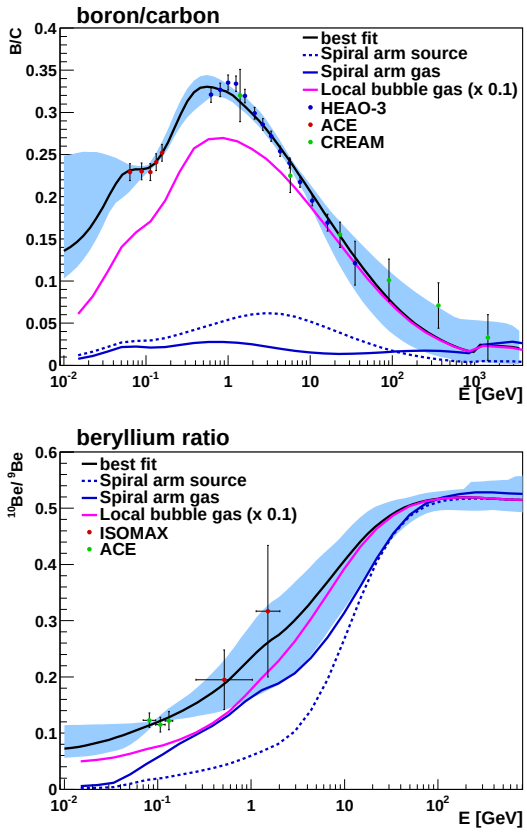

Figure 2: The best fit model for the local B/C (*top*)and $^{10}Be/^{9}Be$ (*bottom*) ratio. Line coding as in fig. 1. Data from HEAO-3 [16], CREAM [17] and ACE [18] for B/C and ISOMAX [19] and ACE [20] for $^{10}Be/^{9}Be$.

the fact that the Sun resides at the edge of a spiral arm, while most secondary CRs are produced in the center of the spiral arms. A comparison between the propagated 1 GeV proton population in the spiral arm model and the propagated 1 GeV proton population in a standard model using the SNR distribution by [22] is shown in fig. 3. Sources distributed along the spiral arms lead to a strong concentration of 1 GeV protons in the inner Galaxy, compared to the reference model. Since the source distribution of the reference model has been tuned to best reproduce the diffuse γ-ray data, this will lead to a very steep radial γ-ray gradient, incompatible with the diffuse γ-ray observations. A smoother radial gradient is obtained if the gas distribution follows the spiral arm structure. It is expected that such a model will help significantly to improve the description of the diffuse γ-ray data. The study of the uncertainties of the spiral arm structure on local CR fluxes and diffuse γ-rays is ongoing, details will be shown elsewhere [23].

2.2 Uncertainties from the local bubble

Our Sun resides in the local bubble (LB), a low density region of space extending about $200-300$ *pc* into the Galactic plane and 600 *pc* perpendicular to it. The density inside the LB is about $0.05\frac{atoms}{cm^2}$, which is approximately a tenth of the average density of the ISM [24]. We have implemented the LB in the 3D DRAGON code. The structure is approximated by a cube with a sidelength of 600 pc. Such scales require resolutions much higher than the commonly adopted 0.5 kpc grid spacing. To minimize computing time a non-equidistant binning has been implemented in the DRAGON code and the optimal bin size with respect to computing time and stability of the numerical solution, has been determined. The lower gas density in the LB leads to lower local energy losses and lower secondary production rates. The latter is of specific interest for the secondary positron flux at high energies, since these positrons are expected to be produced in the local ISM, due to their large synchrotron and inverse Compton losses. The impact of a gas density locally reduced by a factor 0.1 on p, $\bar{p}$, B/C and $^{10}Be/^{9}Be$ is shown in figs. 1 through 2 as the magenta line. In addition to the local gas density, we examined the impact of local variations in the diffusion coefficient (factors 0.25-4) and the Alfven velocity (factors 0.5-2). We find no significant changes in the local proton spectrum and $\bar{p}/p$, B/C and $^{10}Be/^{9}Be$ ratio due to these variations. We also find no significant modulation of the local positron flux due to local variations in the gas density, diffusion coefficient or Alfven velocity above 1 GeV, the found deviations are on the percent level at maximum. This means that the very local transport processes will modify the galactic CR contribution in the positron fraction only marginally. A much stronger impact is expected from the *global galactic* transport parameters, as shown in section 3.

3 Pulsars as sources of high energy electrons and positrons

None of the found models is able to explain the rise in the positron fraction, which steadily increases from 20 to 250 GeV. Previous publications already showed (see e.g. [25]), that this feature is impossible to construct under the assumption of pure secondary production of positrons. It is commonly believed, that an additional source of electron-positron pairs should exist. Here, we model the predicted contribution of 10 nearby pulsars, which are expected to contribute most to the local electron and positron flux on top of the best fit model for the global galactic transport of CRs. The analytic description of the signal is taken from [26], pulsar age, distance, spin-down time, $e^{\pm}$ production efficiency, source spectral index and maximum $e^{\pm}$ energy are taken as fit parameters within their observational limits. Usually an analytic approximation of the energy losses given by only inverse Compton and synchrotron is employed in the literature (see e.g. [26]). Here we use the energy losses and the diffusion coefficient determined by our best fit background model to calculate the pulsar contribution self-consistently[1]. Despite the small impact of the changes of diffusion within the LB on the local secondary e^{+} spectrum found in section 2.2, the diffusion coefficient plays a vital role in the prediction of the local positron fraction: Figure 3 shows our best-fit background model with the additional pulsar contribution. In addition, the limits derived from the two background models with the minimal and maximal diffusion coefficient among the top 100 models are shown. The same variations on the diffusion coefficient have been applied to the pulsar fit, leading to an uncertainty of a factor of about 3 in the signal region.

1. It should be noted that the discrepancy between the analytic description of the energy losses with the numerical values used by [26], results only in discrepancy of a factor of 2 at 10 GeV. For lower energies, where ionization and Coulomb losses become important the factor increases to 10 at 1 GeV.

4 Conclusions

More than 10 million different transport models have been evaluated numerically to constrain the *global galactic* transport model. We showed how the local proton spectrum and the $\bar{p}/p$, the B/C and the $^{10}Be/^{9}Be$ ratios constrain the *global galactic* transport parameters. We find a best fit model with a rather strong increase of the diffusion coefficient with rigidity ($\delta \approx 0.8$), which points to either a non-standard spectrum of turbulence or to an incomplete description of the interplay between CR escape, which is assumed to be energy independent, and CR reacceleration. The galactic wind prefers a coupling to the source distribution $V(R) \propto Q(R)$, as it was found in [7]; the wind strengths determined here are far below those expected from fits to the ROSAT data [8]. We examined the influence of galactic spiral arms and the local bubble on the local CRs. We found the secondary to primary ratios to be extremely sensitive to the spiral arm structure and the exact position of the Sun within this structure, which means that a complete spiral arm model will prefer a completely different point in parameter space than the one found here. This result has a significant impact on the predictions for diffuse γ-rays. Here we presented a first estimate on the additional uncertainties that are to be taken into account for γ-ray production via CR protons. We also showed the uncertainties in the local positron fraction due the global galactic model. A detailed examination of the impact of local variations in the *local* diffusion coefficient and local energy losses and gains, possibly from within the local bubble, is subject to future studies. With the modified DRAGON version we have a powerful tool to study the impact of the very local transport parameters in a realistic scenario. In the light of the upcoming high precision data from AMS-02 these uncertainties and especially the impact on the expected single source anisotropy have to be examined with due care.

Acknowledgment: The authors are grateful to L. Maccione, D. Grasso and D. Gaggero for helpful discussions. Some of the computations were performed on the bw-grid.

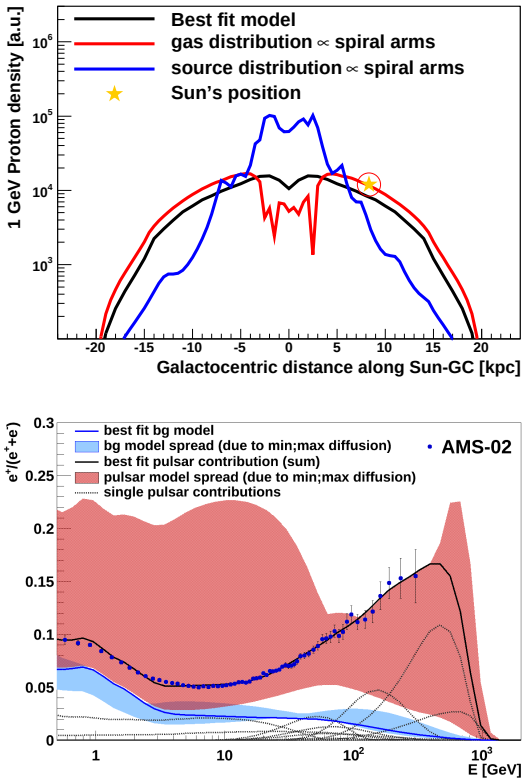

Figure 3: *Top:* The 1 GeV proton distribution versus galactocentric distance along the diameter connecting the Sun and the galactic center (GC). The best fit model obtained in section 2 is shown in black as a reference. The blue line indicates the proton distribution obtained with a model with the source distribution following the spiral arms and the red line is the proton distribution obtained in a model with the gas distribution following the spiral arms. *Bottom:* Contributions of CR electrons and positrons and the contribution of 10 close by pulsars to the positron fraction. The blue line is the background contribution from the best fit model, the blue band indicates the uncertainty from the maximum and minimum diffusion coefficient among the top 100 models. The black line is the total contribution from local pulsars, the red band indicates the uncertainty obtained from the same variation in diffusion coefficient as for the background model.

References

[1] Strong, A. W., Moskalenko, I. V. 2006, http://galprop.stanford.edu/manuals/manual.pdf
[2] http://dragon.hepforge.org/DRAGON/Home.html
[3] Strong, A. W., & Moskalenko, I. V. 1998, The Astrophysical Journal, 509, 212
[4] Gebauer, I. & de Boer, W. 2009, arXiv:0910.2027
[5] Adriani, O., Barbarino, G. C., Bazilevskaya, G. A., et al. 2009, Nature, 458, 607
[6] Aguilar, M., Alberti, G., Alpat, B., et al. 2013, Physical Review Letters, 110, 141102
[7] Breitschwerdt, D., Dogiel, V. A., Völk, H. J. 2002, Astronomy and Astrophysics, 385, 216
[8] Everett, J. E., Zweibel, E. G., Benjamin, R. A., et al. 2008, The Astrophysical Journal, 674, 258
[9] Putze, A., Derome, L., Maurin, D., Perotto, L., & Taillet, R. 2009, Astronomy and Astrophysics, 497, 991
[10] Trotta, R., Jóhannesson, G., Moskalenko, I. V., et al. 2011, The Astrophysical Journal, 729, 106
[11] Liu, Jun S. and Liang, Faming and Wong, Wing Hung 2000, Journal of the American Statistical Association, 95,449
[12] Strong, A. W., Moskalenko, I. V., & Ptuskin, V. S. 2007, Annual Review of Nuclear and Particle Science, 57, 285
[13] I. Gebauer, S. Kunz, in prep.
[14] Adriani, O., Barbarino, G. C., Bazilevskaya, G. A., et al. 2011, Science, 332, 69
[15] Adriani, O., Barbarino, G. C., Bazilevskaya, G. A., et al. 2010, Physical Review Letters, 105, 121101
[16] Engelmann, J. J., Ferrando, P., Soutoul, A., Goret, P., & Juliusson, E. 1990, Astronomy and Astrophysics, 233, 96
[17] Ahn, H. S., Allison, P. S., Bagliesi, M. G., et al. 2008, Astroparticle Physics, 30, 133
[18] Davis, A. J., Mewaldt, R. A., Binns, W. R., et al. 2000, Acceleration and Transport of Energetic Particles Observed in the Heliosphere, 528, 421
[19] Hams, T., Barbier, L. M., Bremerich, M., et al. 2004, The Astrophysical Journal, 611, 892
[20] Yanasak, N. E., Wiedenbeck, M. E., Mewaldt, R. A., et al. 2001, The Astrophysical Journal, 563, 768
[21] Steiman-Cameron, T. Y., Wolfire, M., & Hollenbach, D. 2010, The Astrophysical Journal, 722, 1460
[22] Yuan, Q., Liu, S., & Bi, X. 2012, The Astrophysical Journal, 761, 133
[23] I. Gebauer, M.Weinreuter, S. Kunz, in prep.
[24] Fuchs, B., Breitschwerdt, D., de Avillez, M. A., Dettbarn, C., & Flynn, C. 2006, Monthly Notices of the Royal Astronomical Society, 373, 993
[25] Morselli, A., & Moskalenko, I. V. 2008, Identification of Dark Matter 2008,
[26] Gendelev, L., Profumo, S., & Dormody, M. 2010, Journal of Cosmology and Astrophysics, 2, 16